

8-*N* Rule and Chemical Bonding in Main-Group MgAgAs-type Compounds

David Bende, Frank R. Wagner, Yuri Grin*

*Max-Planck-Institut für Chemische Physik fester Stoffe, Nöthnitzer Straße 40, 01187 Dresden, Germany

Corresponding Author
grin@cpfs.mpg.de

Computational Details

The lattice parameters of the MgAgAs-type compounds were optimized with the PBE functional^[1] and the augmented plane-wave method including local orbitals (APW+lo) as implemented in the Elk code.^[2] The atomic basis functions (except for nitrogen) contain the complete penultimate shell as semi-core states. The program DGrid^[3] was used to obtain quantum chemical real-space bonding indicators. Depending on the sensitivity / expense of the real-space indicators different Elk parameters are used for the SCF cycle (Table S1).

Table S1: Elk calculation parameters for the different types of calculation.

Calculation	k-points	rgkmax	gmaxvr
structure optimization	8 · 8 · 8	9.0	18.0
QTAIM charges and ELI-D	6 · 6 · 6	10.0	20.0
DI calculation	6 · 6 · 6	7.0	12.0

On the appearance of two types of ELI-D topologies for MgAgAs-type main group compounds

While there is always an ELI-D attractor (and a corresponding basin $_{3A',A,E}B$) found between the two most electronegative species A and E, for certain compounds an additional attractor is found between A' and E. Appearance of this second kind of ELI-D attractors (basin $_{A',E}B$) depends on the topology of ELI-D in the vicinity of the three-fold axis running through the E^{HC} and A' positions (Figure S1). There is a ring critical point (RCP) surrounded by three line critical points (LCPs) for the first two compounds in both sequences. The two types of critical points approach each other and finally merge into a maximum which results in the second kind of ELI-D topology (Figure 2, bottom). This is called bifurcation process^[4] which occurs due to the electronegativity and size difference between the components. The ELI-D Laplacian at the LCPs and RCP is negative^[5], i.e. the whole region of the ELI-D distribution in the vicinity of LCP and RPC has bonding character. Therefore, the two ELI-D topologies are the result of a gradual development and do not divide the compounds into two different groups of chemical bonding.

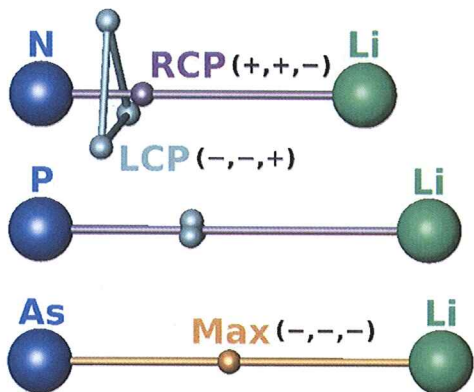
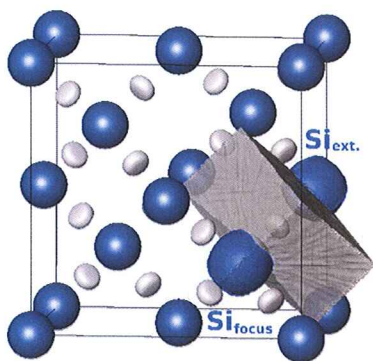


Figure S1: Bifurcation process (inter relation of critical points) in the ELI-D distribution of LiMgN, LiMgP and LiMgAs: RCP - ring critical point, a (3,+1) saddle point; LCP - line critical point, a (3,-1) saddle point; Max - maximum, a (3, -3) attractor. The ELI-D Laplacian at all RCPs and LCPs is negative. Plus and minus indicate the sign of the curvatures in each critical point. A maximum emerges from the unification of RCP and LCPs.

Examples for the calculation of charge claims and connection indices

Example 1: Silicon



The ELI-D topology of silicon in the diamond structure shows four maxima around each core on the connection lines to its nearest neighbors. The four corresponding valence basins are identical and disynaptic and contain $\bar{N}(B_i) = 1.95$ electrons. The number of access electrons per silicon atom is $\bar{N}_{acc}^{ELI}(C^{Si}) = 4 \cdot 1.95 = 7.8$. The various different ELI-D valence basins are contained in the access electron set of one silicon atom. Thus, it is sufficient to calculate the charge claims for one silicon atom to describe the bonding in silicon. The bond fraction with respect to each silicon atom is

$p(B^{Si}) = 0.5$. In order to calculate the genuine and residual charge claims, two different kinds of silicon atoms have to be considered. Si represents the silicon atom which is in the center of the chosen set of ELI-D valence basins i.e. it has a common surface with all four valence basins. Additionally there are four external silicon atoms ($Si_{ext.}$). Each of the external atoms shares surface with one of the chosen valence basins. In terms of the synapticity notation the set of access electron basins reads $\{Si, Si_{ext,1} B; Si, Si_{ext,2} B; Si, Si_{ext,3} B; Si, Si_{ext,4} B\}$. The genuine charge claim and the residual charge claims are calculated as follows:

$$P_{Si}(Si) = \frac{4 \cdot 0.5 \cdot 1.95}{4 \cdot 1.95} = 0.5 \quad (1)$$

$$P_{\text{Si}}(\text{Si}_{\text{ext},1}) = \frac{1 \cdot 0.5 \cdot 1.95 + 3 \cdot 0.0 \cdot 1.95}{4 \cdot 1.95} = 0.125 \quad (2)$$

The residual charge claims of the other external silicon atoms also yield 0.125. The sum over charge claim and the residual charge claims is one. The four external silicon atoms are conceptually and also in the ELI-D/QTAIM intersection picture equivalent (same $P_{\text{Si}}(\text{Si}_{\text{ext}})$). In this case they are summarized.

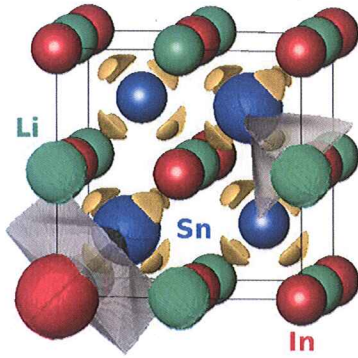
$$P_{\text{Si}}(\text{Si}_{\text{ext,tot}}) = \sum_{i=1}^4 P_{\text{Si}}(\text{Si}_{\text{ext},i}) = 0.5 \quad (3)$$

In order to calculate the connection index CI_{Si} the number of different pairwise interactions has to be identified. Conceptually and in the ELI-D/QTAIM intersection picture as well there is only one kind of covalent bonds in silicon i.e. between two neighboring silicon atoms ($n = 2$). The charge claims of two neighboring silicon atoms are already calculated and so

$$CI_{2\text{Si}} = 4 \cdot [P_{\text{Si}}(\text{Si}) \cdot P_{\text{Si}}(\text{Si}_{\text{ext,tot}})] = 1. \quad (4)$$

It is important to note that the sum of charge claims considered for the evaluation of the connection index is again one. A connection index of one corresponds to a perfect covalent connection of all components within the ELI-D/QTAIM intersection picture.

Example 2: LiInSn



The ELI-D topology of LiInSn in the MgAgAs-type structure shows eight maxima around each tin core on the connection lines to its eight nearest neighbors (4 In + 4 Li). For each tin, four valence basins are identical which makes two different kinds of valence basins. One kind $_{\text{Li,Sn}}B = {}_2B$ has an ELI-D maximum on the Sn-Li connection line, is disynaptic and contains $\bar{N}({}_2B) = 0.41$ electrons. The other kind $_{3\text{Li,In,Sn}}B = {}_5B$ has an ELI-D maximum on the Sn-In connection line, is pentasynaptic and contains $\bar{N}({}_5B) = 1.52$ electrons. The number of access electrons per tin atom is $\bar{N}_{\text{acc}}^{\text{ELI}}(C^{\text{Sn}}) =$

$4 \cdot (0.41 + 1.52) = 7.72$. The various different ELI-D valence basins are contained in the access electron set of one tin atom. Thus, it is sufficient to calculate the charge claims for one tin atom to describe the bonding in LiInSn. The bond fractions of each bonding basin are $p({}_2B^{\text{Li}}) = 0.052$, $p({}_2B^{\text{In}}) = 0.000$, $p({}_2B^{\text{Sn}}) = 0.948$ and $p({}_5B^{\text{Li}}) = 0.002$, $p({}_5B^{\text{In}}) = 0.430$, $p({}_5B^{\text{Sn}}) = 0.564$. The genuine charge claim of the central tin and the residual charge claim of one of the indium atoms are calculated first:

$$P_{\text{Sn}}(\text{Sn}) = \frac{4 \cdot 0.948 \cdot 0.41}{7.72} + \frac{4 \cdot 0.564 \cdot 1.52}{7.72} = 0.646 \quad (5)$$

$$P_{\text{Sn}}(\text{In}_1) = \frac{4 \cdot 0.000 \cdot 0.41}{7.72} + \frac{1 \cdot 0.430 \cdot 1.52 + 3 \cdot 0.000 \cdot 1.52}{7.72} = 0.085 \quad (6)$$

The first term in equation 5 and 6 refers to the disynaptic basins, the second term to the pentasynaptic basins. The residual charge claims of the remaining three indium atoms are identical: $P_{\text{Sn}}(\text{In}_1) = P_{\text{Sn}}(\text{In}_2) = P_{\text{Sn}}(\text{In}_3) = P_{\text{Sn}}(\text{In}_4)$. This equivalence as well as their conceptual equivalence allows the four indium atoms to be summarized according to

$$P_{\text{Sn}}(\text{In}_{\text{tot}}) = \sum_{i=1}^4 P_{\text{Sn}}(\text{In}_i) = 0.34 \quad (7)$$

Each lithium atom contributes electrons to four ELI-D basins within the access electron set of tin: One disynaptic basin and three pentasynaptic basins.

$$P_{\text{Sn}}(\text{Li}_1) = \frac{1 \cdot 0.052 \cdot 0.41}{7.72} + \frac{3 \cdot 0.002 \cdot 1.52}{7.72} = 0.0035 \quad (8)$$

The charge claims of the four lithium atoms are equivalent: $P_{\text{Sn}}(\text{Li}_1) = P_{\text{Sn}}(\text{Li}_2) = P_{\text{Sn}}(\text{Li}_3) = P_{\text{Sn}}(\text{Li}_4)$. The four lithium atoms are summarized for the same reasons as the indium atoms:

$$P_{\text{Sn}}(\text{Li}_{\text{tot}}) = \sum_{i=1}^4 P_{\text{Sn}}(\text{Li}_i) = 0.014 \quad (9)$$

The sum over the charge claims of the three components is one. In order to calculate the connection index CI_{Sn} the number of different pairwise interactions has to be identified. Within the ELI-D/QTAIM intersection picture all three components participate in the ELI-D valence basins ($n = 3$). It is important to note that the sum of charge claims considered for the evaluation of the connection index is again one.

$$CI_{\text{Sn}} = 3 \cdot [P_{\text{Sn}}(\text{Sn}) \cdot P_{\text{Sn}}(\text{Li}_{\text{tot}}) + P_{\text{Sn}}(\text{Sn}) \cdot P_{\text{Sn}}(\text{In}_{\text{tot}}) + P_{\text{Sn}}(\text{Li}_{\text{tot}}) \cdot P_{\text{Sn}}(\text{In}_{\text{tot}})] = 0.700. \quad (10)$$

The deviation from the ideal value of one mainly originates from the lithium atoms which are almost completely excluded from covalent interactions.

On the similarity of the two direct-space bonding measures

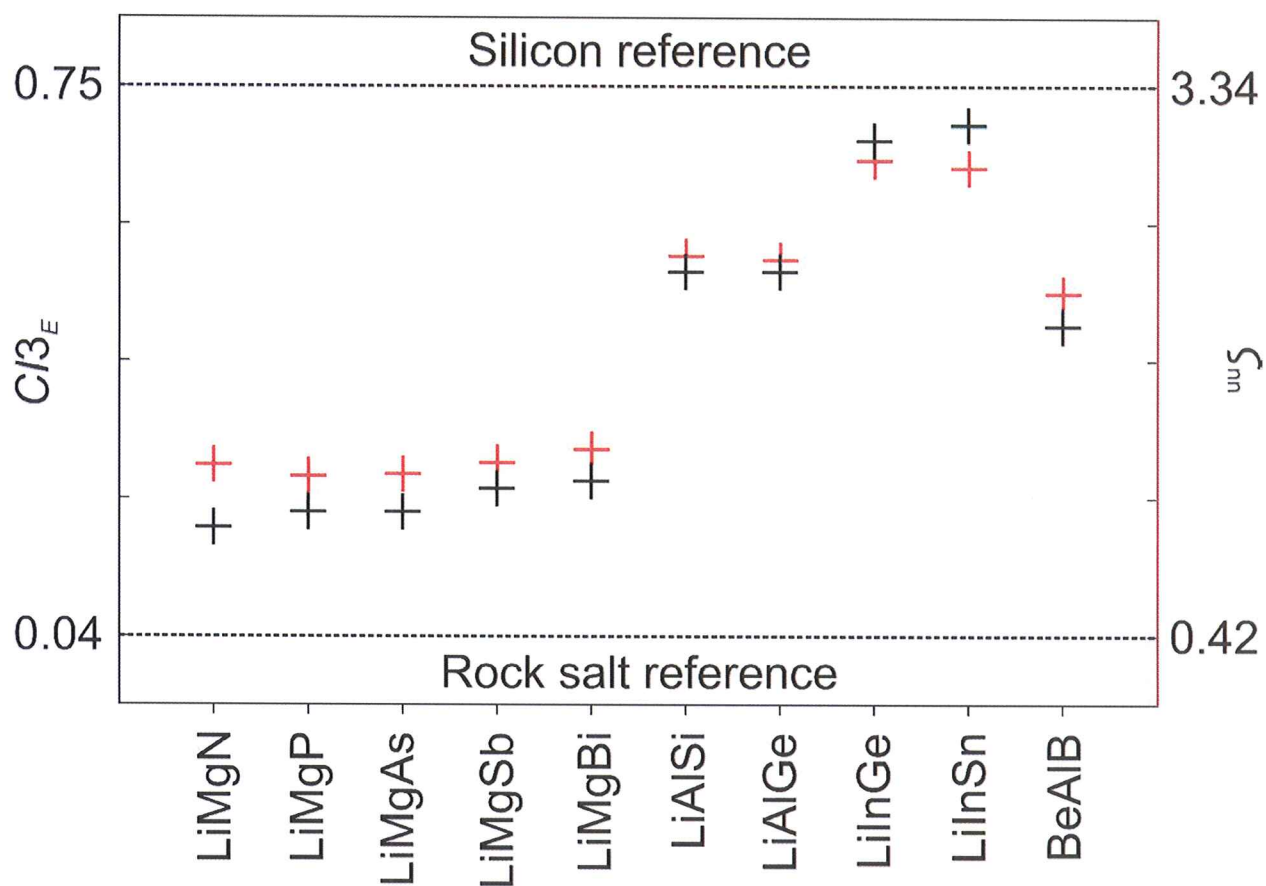


Figure S2: Connection index CB_E (black crosses) and nearest neighbor sharing s_{nn} (red crosses) for $A'AE$ compounds in the context of the two reference compounds rock salt (ionic bonding) and silicon (covalent bonding). The more realistic scale compared to the conceptual values in Figure 5 for both bonding measures leads to smaller and more uniform deviations between CB_E and s_{nn} .

Table S2: Direct-space bonding properties of some zinc-blende-type and anti-fluorite-type compounds as they appear in Figure 7. $\bar{N}_{acc}^{ELI}(C^E)$: ELI-D access electrons of E; P: charge claim; N_{lp} : number of lone pairs (according to the presented formalism); $\bar{N}_{val}^{ELI}(E)$: ELI-D valence electrons of E; CIn_E : Connection index.

AE	GaAs ^[6]	InSb ^[7]	AlP ^[8]	BN ^[9]	BeS ^[10]	Li ₂ S ^[11]	Mg ₂ Si ^[12]	Na ₂ S ₂ ^[13]	NaP ^[14]	LiSi ^[15]
$\bar{N}_{acc}^{ELI}(C^E)$	8.48	7.88	7.84	7.80	7.84	7.84	7.76	7.33	7.37	7.68
$P_E(E) / \%$	69	71	88	89	95	97	87	92	78	62
$N_{lp}(E)$	1.61	1.65	2.98	3.04	3.53	3.68	2.87	3.08	2.06	0.92
$\bar{N}_{val}^{ELI}(E)$	5.85	5.63	6.89	6.93	7.50	7.60	6.73	6.77	5.78	4.73
$Q^{eff}(E)$	-0.62	-0.44	-1.97	-2.06	-1.57	-1.68	-2.80	-0.84	-0.85	-0.82
$CIn_E / \%$	86	82	42	39	19	12	45	19	48	65

References

- (1) Perdew, J. P.; Burke, K.; Ernzerhof, M. *Phys. Rev. Lett.* **1996**, *77*, 3865-3868.
- (2) Program Elk, version 1.4.22, www.elk.sourceforge.net.
- (3) Kohout, M. DGrid, version 4.7, Radebeul, **2013**.
- (4) Bader, R. F. W. in *Atoms in Molecules*, Oxford University Press, Oxford, 1990.
- (5) Wagner, F. R.; Kohout, M.; Grin, Yu.; *J. Phys. Chem. A* **2008**, *112*, 9814-9828.
- (6) Goldschmidt, V. M. *Skr. Nor. Vidensk.-Akad.* **1926**, 8-1.
- (7) Goldschmidt, V. M.; Barth, T.; Lunde, G.; Zachariasen W. H. *Skr. Nor. Vidensk.-Akad.* **1926**, 2-1.
- (8) Passerini L. *Gazz. Chim. Ital.* **1928**, *58*, 655-664.
- (9) Wang C. C. *Diss. Abstr.* **1963**, *23*, 3154-3155.
- (10) Staritzky E. *Anal. Chem.* **1956**, *28*, 915.
- (11) Zintl, E.; Harder, A.; Dauth, B. Z. *Elektrochem. Angew. Phys. Chem.* **1934**, *40*, 588-593.
- (12) Bol'shakov K.A.; Bul'onkov N.A.; Rastorguev L.N.; Tsirlin M.S.; *Russ. J. Inorg. Chem.* **1963**, *8*, 1418-1421.
- (13) Föpl, H. *Angew. Chem.* **1958**, *70*, 401.
- (14) Hönle W.; Von Schnering H.G. *Acta Crystallogr. A* **1978**, *34*, S152.
- (15) Evers J.; Oehlinger G.; Sextl G. *Eur. J. Solid State Inorg. Chem.* **1997**, *34*, 773-784.